PHOTOCATHODES TESTED IN THE DC GUN OF THE CERN PHOTOEMISSION LABORATORY

E. Chevallay, J. Durand, S. Hutchins, G. Suberlucq, M. Wurgel

Abstract

In the framework of the CERN Linear Collider project (CLIC) the CLIC Test Facility (CTF) uses a laser driven photocathode in an RF gun as an electron source. Photocathodes properties are measured in the Photoemission Laboratory, which consists of a preparation chamber and a DC electron gun, followed by a beam measurement line. Cathodes are illuminated by a nanosecond UV YAG laser.

The present note concerns the present installation and resumes different photocathode tests on metallic as well as alkali cathodes. Those used in the RF gun of the CTF are particularly emphasized.

Photocathodes Tested in the DC Gun
of the CERN Photoemission Laboratory

E. Chevallay, J. Durand, S. Hutchins, G. Suberlucq, M. Wurgel
CERN — PS Division, 1211 Geneve 23, Switzerland

In the framework of the CERN Linear Collider project (CLIC) the CLIC Test Facility (CTF) uses a laser driven photocathode in an RF gun as an electron source. Photocathode properties are measured in the Photoemission Laboratory, which contains a preparation chamber and a DC electron gun, followed by a beam measurement line. Cathodes are illuminated by a nanosecond UV YAG laser. The present note concerns the present installation and summarises different photocathode tests on metallic as well as alkali cathodes. Those used in the RF gun of the CTF are particularly emphasized.

1. Introduction

The studies started at CERN on a two-beam linear collider under the title of CERN LInear Collider (CLIC) cover different subjects [1]. A CLIC Test Facility (CTF) is used [2] to study the generation of high intensity (kA), picosecond-length electron bunches. These bunches are used to generate 30 GHz RF power. The electron source is a 3 GHz RF gun equipped with a laser driven photocathode. In order to provide the most suitable cathode for the CTF RF gun, different kinds of cathodes are developed and studied in the photoemission laboratory. This contains an evaporation chamber where photocathodes are produced, then inserted under vacuum into a high voltage DC gun, where they are illuminated by nanosecond laser pulses of visible and UV light. An electron beam measurement line is used to determine
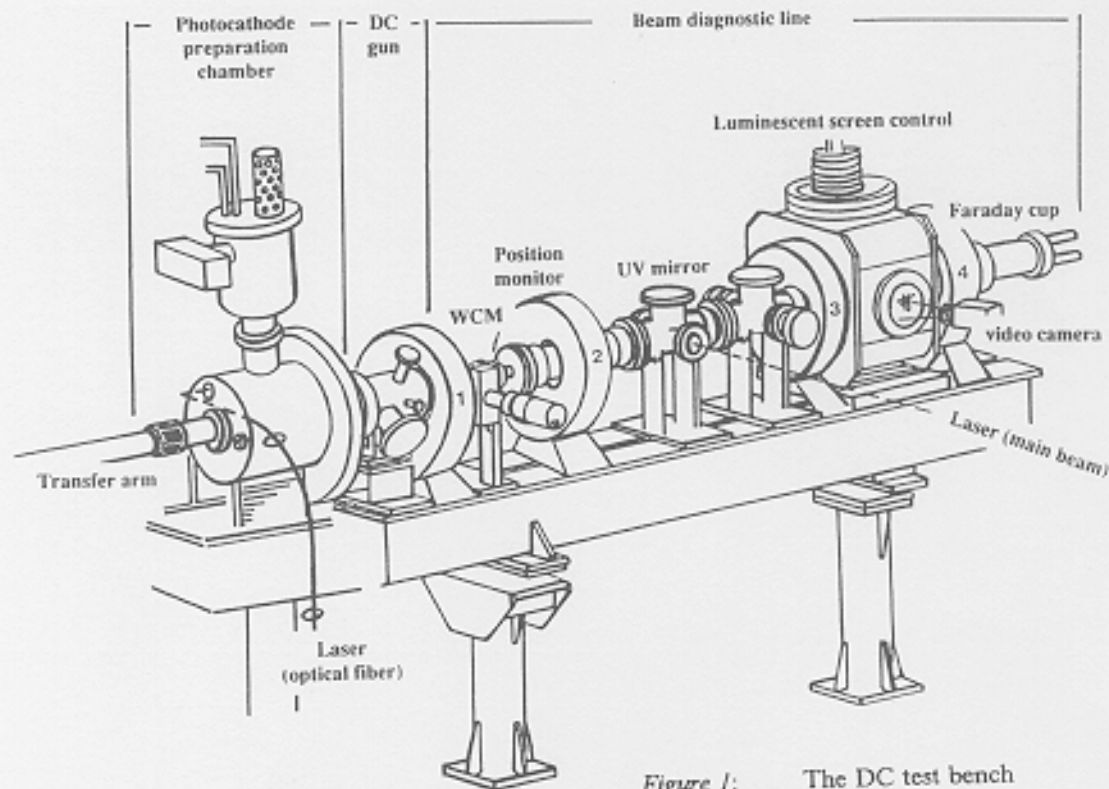

Figure 1:   The DC test bench

the photocathode properties. These different parts are called the DC Test Bench [3].

2. Description of the installation

A general view of the DC Test Bench is shown on Figure 1.

2.1 The preparation chamber

Two different processes are available in the preparation chamber, the evaporation process and cleaning by glow discharge. The preparation chamber is able to evaporate three different products, separately, or simultaneously. During evaporation, the pressure rises from a few 10^{-10} mbar up to about 2×10^{-7} mbar, depending on the type of evaporated product. The layer thickness is estimated by measuring the frequency change induced by the increased mass of a quartz crystal exposed to the metal vapour. During the evaporation process the cathode is illuminated by UV nanosecond laser pulses at either 266 nm or 355 nm via an optical fiber, and the electrons emitted are collected on a biased electrode, in front of the cathode. The distance between the cathode and the sources is 12 cm and a fast shutter is able to mask the cathode from the metal vapour. Up to now, the cathode heat-ing process has not been available and the evaporation process has been with the cathode at ambient temperature. The process is monitored by a PC which regulates the heater power for each evaporation product boat. It is also possible to reproduce automatically some evaporation sequences [4]. Figure 2 shows a typical evaporation process, in this case, production of a K_3Sb cathode.

In the same chamber, but not at the same time, it is possible to clean the surface of the cathode by Ionised Controlled Etching (ICE), which is a glow discharge of Argon ions. The plasma is confined by a magnetic field and controlled by a regulated argon pressure system at 5×10^{-2} mbar[5].

2.2 The DC gun

The gun consists of two parallel electrodes, separated by a gap of 1 cm and subjected to a maximum potential difference of 100 kV (usually 80 kV). The cathode body contains a photocathode plug with a 12 mm diameter photoemissive surface. The anode has a hole of 16 mm diameter for electron and photon beam transmission. A theoretical model of the gun is given in [3], and some parameters are listed on Table 1 for 80 kV.
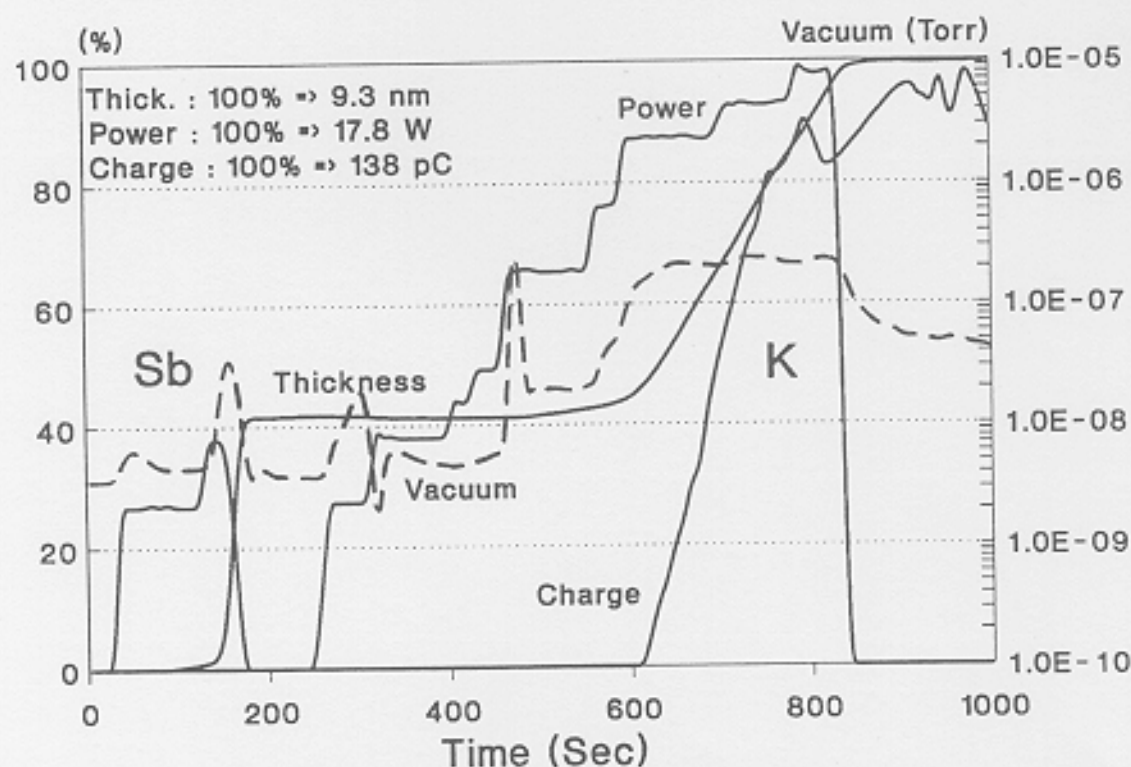

Thick. : 100% => 9.3 nm
Power : 100% => 17.8 W
Charge : 100% => 138 pC

Figure 2: K_3Sb cathode, evaporation process

2.3 Lasers

The type of laser chosen for the CTF is a Nd:YLF mode-locked oscillator and amplifier, due to the requirements for short pulses and timing stability with respect to the RF phase in the cavity. The fundamental wavelength used is 1047 nm, the corresponding photon energy is only 1.1 eV which is insufficient for any of the photocathode materials of interest. By harmonic generation in non-linear materials, photon energies of up to 6 eV (fifth harmonic) are attained, enabling the use of several different types of photocathode. In the Photoemission Laboratory a nanosecond-pulse Nd:YAG laser is used with a fundamental wavelength of 1064 nm, and harmonic generation to provide several wavelengths for tests, close to those available in the CTF. Photocathodes have been tested at several wavelengths by different types of laser, their parameters are listed below (Table 2).

λ the wavelength delivered by the laser
τ the Full Width Half Maximum pulse duration
Frep the repetition rate
S the area of the laser spot which contains 86 % of the energy
Wcath the effective energy on the photocathode

Nd:YAG Neodymium:YAG laser, Spectron Laser Systems SL-400
XeCl Xenon Chloride excimer laser, Lambda Physik EMG101
ArF Argon Fluoride excimer laser from Sopra.
Nd:YLF picosecond Neodymium:YLF laser from Quanta System, only the fifth harmonic is at present used at the CTF experiment. The pulse delivered by the laser can be split into 8 micro-pulses with a distance of 333 ps between pulses.

The laser energy was measured by a pyroelectric joulemeter with an accuracy of better than ±5 % over the wavelengths cited.

2.4 The electron beam measurement line

The focusing is provided by four air-cooled solenoids. Focal lengths of 10 cm can be achieved with about 2 amps in the coils [3]. Just after the gun, the intensity and the time distribution of the electron beam are measured by a Wall Current Monitor (WCM) (see Figure 1). Electronic integration of this signal gives the charge of the beam [6]. Next, an

Table 2: Laser parameters

	λ nm	τ ns	**Frep.** Hz	**S** mm^2	**Wcath.** μJ
Nd:YAG	213	6	10	10	$\leq$25
	266	6	10	1$\leq$S$\leq$40	$\leq$300
	355	6	10	10	$\leq$1200
	532	6	10	10	$\leq$2000
XeCl	308	15	2.5	40	$\leq$2000
ArF	193	15	1	28	$\leq$100
Nd:YLF	209	0.014	10	25	$\leq$15

electrostatic pick-up with a bandwidth of 700 MHz measures the relative position of the beam barycentre with an accuracy of ±0.5 mm. The electrons then encounter a retractable fluorescent screen, which is used for initial adjustments of the focusing coils as well as image analysis of the electron beam transverse profiles. At the end of the line, charge measurements are made with a Faraday cup [7]; the charge measurement accuracy is better than ±5 % for both charge detectors. Coupled with the acquisition from the Faraday cup, a motorised x-y mirror support enables automatic scanning of the cathode surface [8].

3. CTF photocathode requirements

Theoritical considerations and first experiments in CTF [9] have demonstrated some limitations of the laser optics and photocathodes. The use of the fifth harmonic and photocathodes in CsI has been a valuable first step, but the conversion efficiency to this wavelength (209 nm) is low, only 100 μJ laser energy is available for 10 mJ at the fundamental wavelength. Also the practical difficulties in the production of UV optics reduce the efficiency of transporting this energy to the cathode [10]. Operation at a longer wavelength increases the amount of energy available, the stability of the laser and the efficiency with which the light may be brought to the cathode. For these reasons it was decided to use a wavelength longer than 250 nm, therefore the Quantum Efficiency (QE= ratio of output electrons to incident photons) must be higher than or equal to 1 %. The relaxation time (the time to convert and extract all electrons produced by photons) should be lower than a few picoseconds. The photocathode lifetime (time to decrease from QE_{max} to the half value) should be

longer than a week with an electric field higher than or equal to 100 MV/m and a laser intensity of 5 MW/cm^2. Finally, under these conditions, the cathode must be able to deliver 12 nC/pulse with a current density close to 3.3 kA/cm^2.

4. Metallic photocathodes

Initially, metallic cathodes appeared the easiest to produce and use. They have the fastest relaxation times and surfaces capable of withstanding the intense fields. Practically, however, we observe some difficulties. Metallic cathodes have low quantum efficiency of a few 10^{-4}, because emitted electrons come only from few atomic layers and the reflectivity of the surface is generally high. Metals have high work functions of 4 or 5 eV, consequently, the wavelength of the laser must be short. Only pure metals have reproducible characteristics; when exposed to air, without further vacuum cleaning treatment, the surface becomes oxidised and its photoemissive properties are affected. Nevertheless, it should be possible to obtain high current densities with femtosecond laser pulses [11] and multi-photon process [12]. Table 3 lists quantum efficiencies, measured in our laboratory at different wavelengths (expressed in nm and in the corresponding eV) for different metals. For each, the work function ϕ_s is given [13].

WK$^+$ is a special Tungsten cathode doped with Potassium by ion implantation at the University of Lyon (F). The implantation energy was 150 keV, the ion density 1.3×10^{17} ions/cm^2, and the resulting Potassium concentration was 30 % [14]. Figure 3 shows the QE as a function of the cleaning process.

Table 3: Metallic cathodes : QE = f(λ)

λ (nm)	193	213	266	308	355	ϕ_s
E (eV)	6.42	5.82	4.66	4.03	3.49	eV
Al		8.4×10^{-4}	3.2×10^{-5}		3.4×10^{-7}	4.3
Au		4.0×10^{-4}	1.3×10^{-5}			5.1
Cu	2.0×10^{-4}	1.5×10^{-4}	2.2×10^{-6}	1.6×10^{-7}	8.0×10^{-9}	4.6
Cu **	1.5×10^{-3}	4.2×10^{-4}				4.6
St steel		9.0×10^{-5}	1.6×10^{-6}			
Sm				1.6×10^{-6}		2.7
Y			2.7×10^{-6}	1.1×10^{-6}		3.1
Y **			1.8×10^{-4}			3.1
WK$^+$ **				1.2×10^{-5}		2.8

** = ICE cleaning process under vacuum

We observe a "Potassium tank" effect: after reaching a maximum the QE decreased as the etched depth increased. Left for 90 hours, ions migrated to the surface, and the QE increased by a factor of four [15].
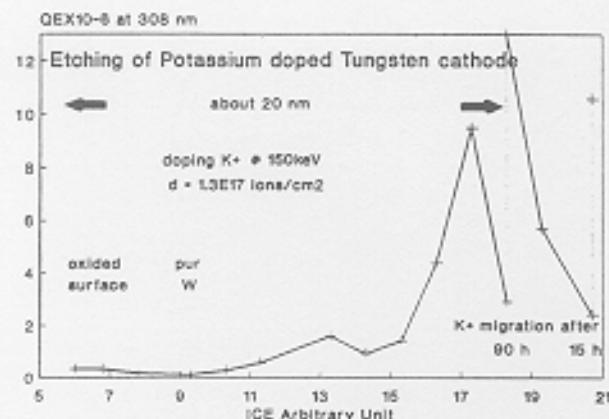

QEX10-6 at 308 nm

Etching of Potassium doped Tungsten cathode

about 20 nm

doping K+ ≈ 150keV
d = 1.3E17 ions/cm2

oxided
surface

pur
W

K+ migration after
90 h   16 h

ICE Arbitrary Unit

Figure 3:

WK$^+$: QE = f(etching).
Arbitrary etching unit : U_{plasma} = 800 V
P_{argon} = 5.8×10^{-2} mbar
time = 40 minutes

In the CTF we started with copper cathodes for RF gun studies and electron beam line set-up. We found quantum efficiencies of about 3×10^{-4}, an intermediate value between normal and ICE cleaned copper; indicating a cleaning effect in the RF gun, by high electric field (100 MV/m), or high laser power density, or both. The behaviour in the RF gun was roughly as expected [16].

In all metallic cathodes the QE is unfortunately too low. For this reason we have tried other kinds of photocathodes, particularly the alkalis.

5. Alkali photocathodes

There are two different groups: alkali antimonides and alkali halides. The second group works only in the UV light range, but they are well known as being less sensitive to air exposure than the antimonide group. This was an important factor in our installation.

In alkali photocathodes, electrons come from the valence level. For electrons to escape, photons must deliver enough energy to raise the electron from the valence to the conduction band (E_g) and from conduction band to vacuum level (E_a): $E_{photon} \geq E_g + E_a$, for a single photon process.
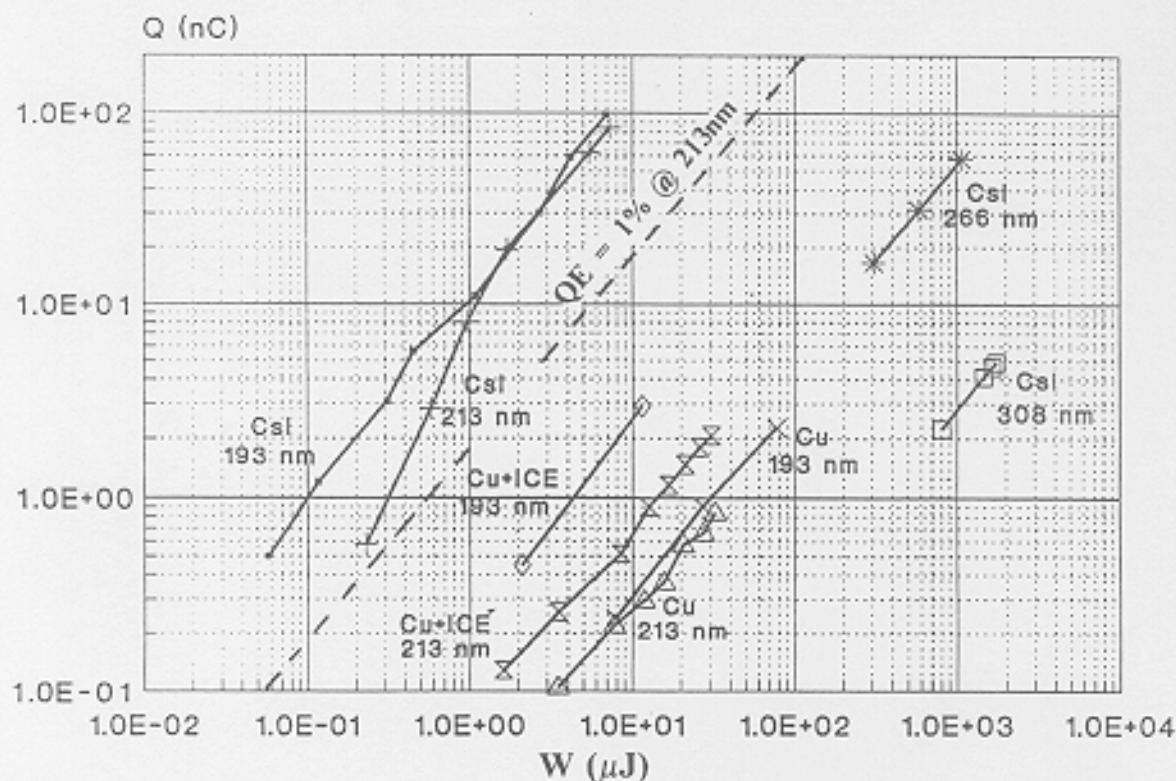

Figure 4:   CsI,Cu : Q = f(w)

5.1 Caesium iodide photocathode

This is an alkali halide photocathode; $E_s = 6.3$ eV, and $E_a = 0.1$ eV [17]. Due to lack of a transport chamber, photocathodes cannot be yet transferred now under vacuum, from the preparation chamber to the CTF. For this reason we have used Caesium iodide cathodes, due to their resistance to air exposure for a short time. Measurements of these photocathodes are reported in [18]. To reduce the influence of the substrate and to increase the adhesion between layers, we have vacuum deposited a 100 nm aluminium layer, prior to evaporating 350 nm of CsI (from Merck, of 99.5 % purity) [19]. Main results are shown in figures 4 to 7, both from the photoemission lab and in the CTF.
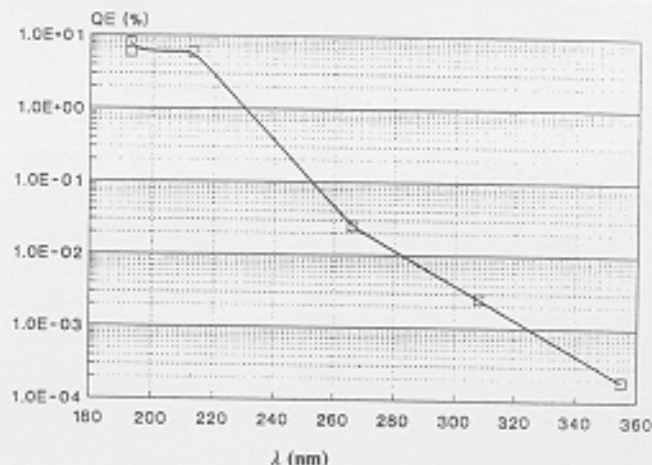
Fig 4 Charge as a function of the laser intensity for CsI and copper cathodes. In surface photoemission processes, the multiphotonic order is indicated by the slope of these curves. We observe a slope of one indicating a single photon process, except for CsI at 213 nm, which is close to Ea + Eg. At this wavelength the slope is a function of the laser intensity, and the charge is not limited by gun saturation. The slope of two, at 213 nm was reported at the Brookhaven National Laboratory [20].

Figure 6:   CsI : QE = f(λ)

Fig 6 Quantum efficiency of CsI cathodes versus wavelength. The photoemission cut-off is at

$$\lambda_c = \frac{1239.8}{E_a + E_s} \approx 194nm.$$ We have observed a longer cut-off wavelength, close to 220 nm.
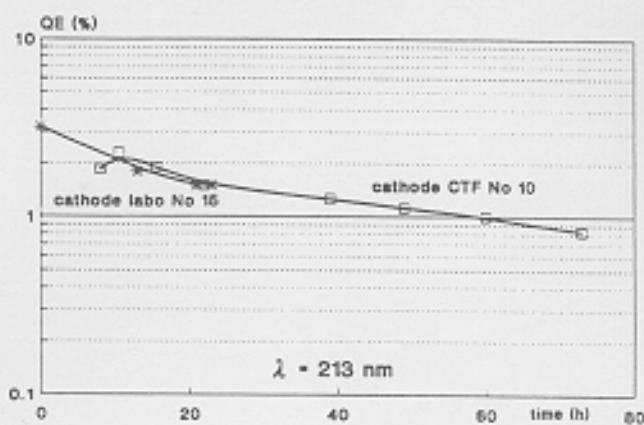
350nm CsI on 100nm Al base

Figure 7:   CsI lifetime

Fig 7 Lifetime of CsI cathodes: due to better conditions during the evaporation process, the lifetime now is longer than is indicated on this curve. More than one week of continuous work with high voltage and laser is possible for a decrease to half the initial QE.

Q measurements on WCM

1 : 213nm (350nm)   2 : 193nm (350nm)   3 : 193nm (700nm)
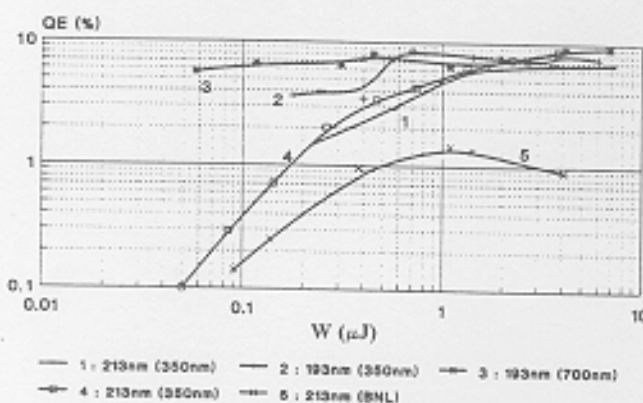4 : 213nm (350nm)   5 : 213nm (BNL)

Figure 5:   CsI : QE = f(w)

Fig 5 Quantum efficiency of CsI cathodes versus laser intensity. $QE \approx \dfrac{1.24 \times Q_{nC}}{W_{\mu J} \times \lambda_{nm}}$. We observe the slope change above an energy density of 3 $\mu J/cm^2$ at 213 nm.

In the CTF, at 209 nm, we have observed the same behaviour at low energy as was observed in the photocathode laboratory. Above a laser energy density of 5 $\mu J/cm^2$, not all electrons liberated are extracted from the gun in one RF cycle and a bunch train appears. It is not understood why this occurs.

The time between these bunches is one RF period of 333 ps. When the laser pulse is divided into eight micro-pulses at one RF wavelength distance, the CsI cathode starts to saturate before the RF gun saturation. The total charge produced in 8 pulses is only 68 % of the sum of charges produced by each individual pulse. We have observed a time dependence of this saturation. The peak QE was 7.8 %, close to values measured in the lab. The working point for the better CTF behaviour with this cathode, requires an RF phase where all electron produced are not extracted, and the corresponding apparent QE is only 2 % [16].

At this wavelength, we have experienced difficulties with the laser and the optical path due to the technical problems of manufacturing UV optics. For these reasons added to the unexpected behaviour of the CsI cathode in the RF gun (saturation and satellite bunches), we have decided to carry out research on other alkali cathodes.

5.2 Caesium telluride photocathode

This is also an alkali halide, whose characteristics are less well defined than the previous CsI cathode. Depending on the author, [17], [21], [22], [23], the electron affinity and the valance gap have quite different values. Nevertheless, we can assume: $3.7 \text{ eV} \leq E_g \leq 4.5 \text{ eV}$ with few tenths of one eV for E_a. As in CsI cathodes, the large ratio of E_g to E_a does indicate a large QE for wavelengths shorter than 275 nm, which is the right value for the fourth harmonic of a YAG or YLF Neodymium laser. This alloy has a lower resistivity than CsI, and good behaviour under high electric field with very low values of dark current [24], [22]. The stoïchiometric ratio suggests a layer of Caesium seven times the Tellurium thickness, however we observed a maximum quantum efficiency with approximately 18 nm of Caesium over 10 nm of Tellurium. We conclude that only a small portion of the Tellurium reacts with the Caesium, probably because we do not heat the substrate during the evaporation process. We have tried different evaporation processes, such as "yoyo" (many thin alternate layers of the two materials), but the simplest process, one layer of Caesium on one layer of Tellurium, gave the best result. The evaporation pressure was about 10^{-8} mbar. In all cases the Caesium thickness was optimized at 266 nm laser wavelength, by measuring photoemission during the evaporation.

We have made different Cs_2Te cathodes, preparation conditions are summarised below, and measurements are presented from the Figure 8 to the Figure 11

Cs_2Te No1 Te: 8.2 nm, and after Cs: 7.1 nm, on a stainless steel substrate.

Cs_2Te No2 Te: 10 nm, Cs: 19.4 nm, and an estimated thickness of 38 nm of Cs and Te evaporated simultaneously.

Cs_2Te No3 Deposited on the previous cathode, in a "yoyo" process of 10 cycles, alternately one or two nanometers of Te and Cs.

Cs_2Te No4 Te: 10.2 nm, Cs: 18 nm, on a stainless steel substrate.

Coleman photocathode described in reference [21]
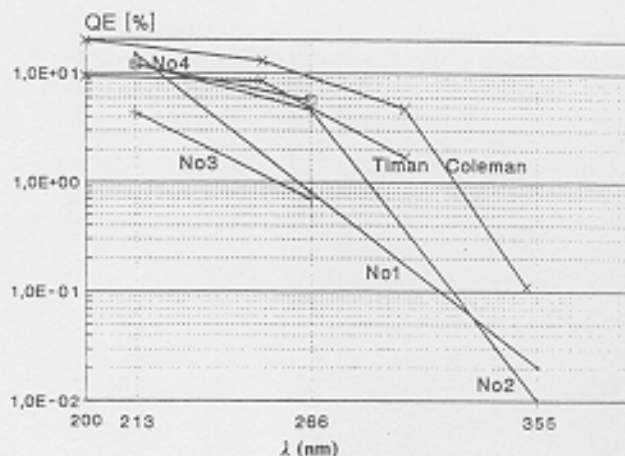
Timan photocathode described in reference [23]

Figure 8: $Cs_2Te : QE = f(\lambda)$

Fig 8 Spectral response of different cathodes prepared in the laboratory compared to some produced in 'solar blind' photomultipier applications. We have observed a shorter cut-off wavelength than expected, but still compatible with the fourth harmonic of YAG or YLF Neodymium laser.
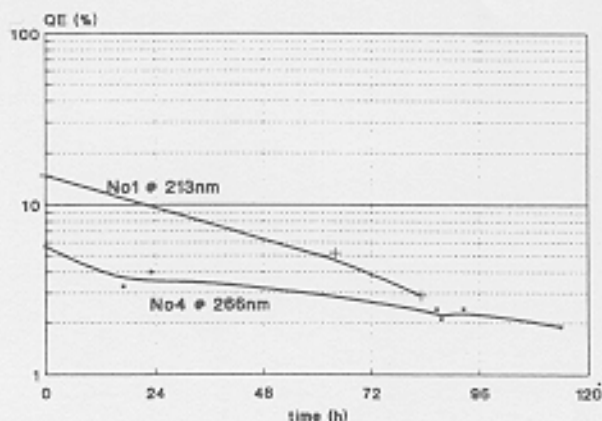

Figure 9: Cs_2Te lifetime

Fig 9 The lifetime of the Cs$_2$Te No1 was measured at 213 nm, and without high voltage or laser for the first 64 hours and with both during the 19 hours following. For the Cs$_2$Te No4 cathode, the quantum efficiency was measured with 2 μJ at 266 nm and 80 kV on the cathode permanently. The lifetime is close to 60 h, and QE remains higher than 1 % for more than one week.

Cs2TE No4
QE = 3.3% @ X=Y=0 and lambda = 266 nm
ceth. diam.= 9mm ; laser beam diam. 4mm
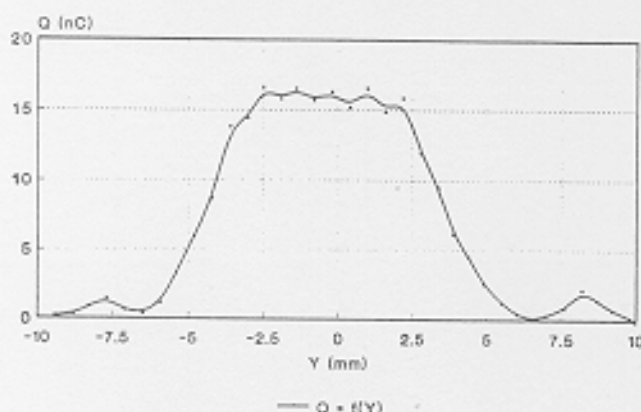
Q (nC)

Y (mm)

— Q = f(Y)

Figure 10:   Cs$_2$Te homogeneity

Fig 10 We can see the homogeneity of the cathode emitted charge along the y-axis. This measurement was done after 45 hours of continuous working (see Fig. 9), with a 4 mm diameter laser beam on a 9 mm sensitive area of the Cs$_2$Te No4 cathode.

Cs2Te No4
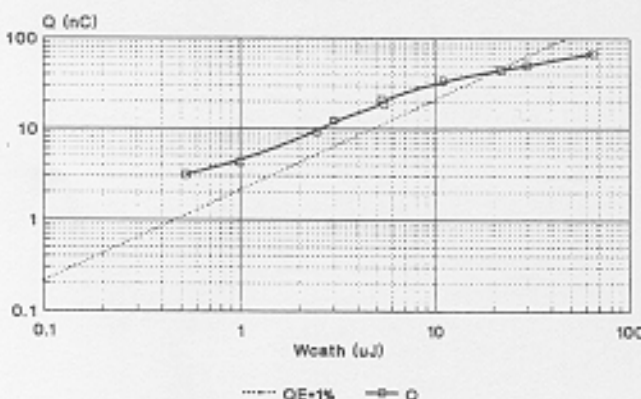measurements after 120h
laser beam : 2mm diam.

Q (nC)

Wcath (uJ)

···· QE=1%   —⊟— Q

Figure 11:   Cs$_2$Te : Q = f(w)

Fig 11 This figure shows the emitted charge versus laser energy after more than 4 million laser shots with an electric field of 8 MV/m. In order to compare the behaviour of CsI and Cs$_2$Te cathodes, measurements were done with a 2 mm diameter laser beam. Only gun saturation due to space charge effect was observed for density energy from 0.3 mJ/cm^2 to 2.2 mJ/cm^2 as expected.

To test the influence of exposure to air we simulated, after a lifetime test, an air transfer of the Cs$_2$Te No4 cathode from the photoemission lab to CTF. As shown in Figure 12, the QE decreased by a factor of 200 at 266 nm. In the Photocathode lab, we tried to regenerate the cathode by etching the surface to suppress oxidised layers. Using both focused laser pulses and DC high voltage it was possible to rejuvenate the cathode, the QE rose by two orders of magnitude (see Figure 12). Unfortunately it is difficult to control this process, which used in the CTF with an RF electric field, destroyed the cathode. Nevertheless, in the CTF at 209 nm, the same QE as in the laboratory was obtained (0.3 %), after exposure to air. We have observed a very low dark current in the lab as well as in the CTF.
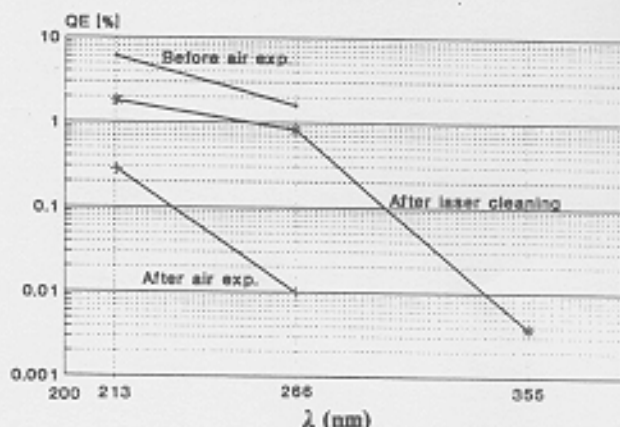

Cs2Te No4
After 5E6 laser pulses

QE [%]

Before air exp.

After laser cleaning

After air exp.

λ (nm)

Figure 12:   Cleaning of a Cs$_2$Te cathode

Since the rejuvenation of a Cs$_2$Te cathode with focused laser and high voltage was not conclusive in the CTF, and to avoid the problem of air contamination we need to transport the photocathode under vacuum from the photoemission laboratory to the CTF. Figure 13 shows the equipment under construction or modification to produce, test, transport under vacuum, and finally insert the photocathode in the RF gun.

Up to four cathodes can be manually loaded on the Manipulator Photocathode MPC-3. This operation is done under Nitrogen flow and is immediatly pumped down. The vacuum system of the Transport Carrier also pumps down the intermediate volume at each connection.

Using the Connecting Flanges, the Transport Carrier is connected to the Transit Chamber in the Photoemission Laboratory, and a cathode is transferred from MPC-3 to MPC-1. Then, MPC-1 pulls it into the preparation chamber. The Cs_2Te photoemissive thin film is deposited. MPC-1 pushes it into the DC gun for photoemission measurement. Finally, it is stored back into the Transport Carrier through the Transit Chamber. The whole process is repeated for each cathode.

At the CTF, any of the four photocathodes can be transferred and plugged into the RF gun via the RF gun Transfer Chamber, using MPC-3 and MPC-2.

5.3 Alkali photocathodes summary

We produced and tested alkali antimonide cathodes as described by A.H. Sommer[17]. In general we observed a good efficiency, cut-off wavelengths shorter than expected, and very short lifetimes. As expected the influence of the vacuum quality was observed, both on the QE and the lifetime of the cathodes. The Table 4 summarises the quantum efficiencies against wavelength of alkali photocathodes
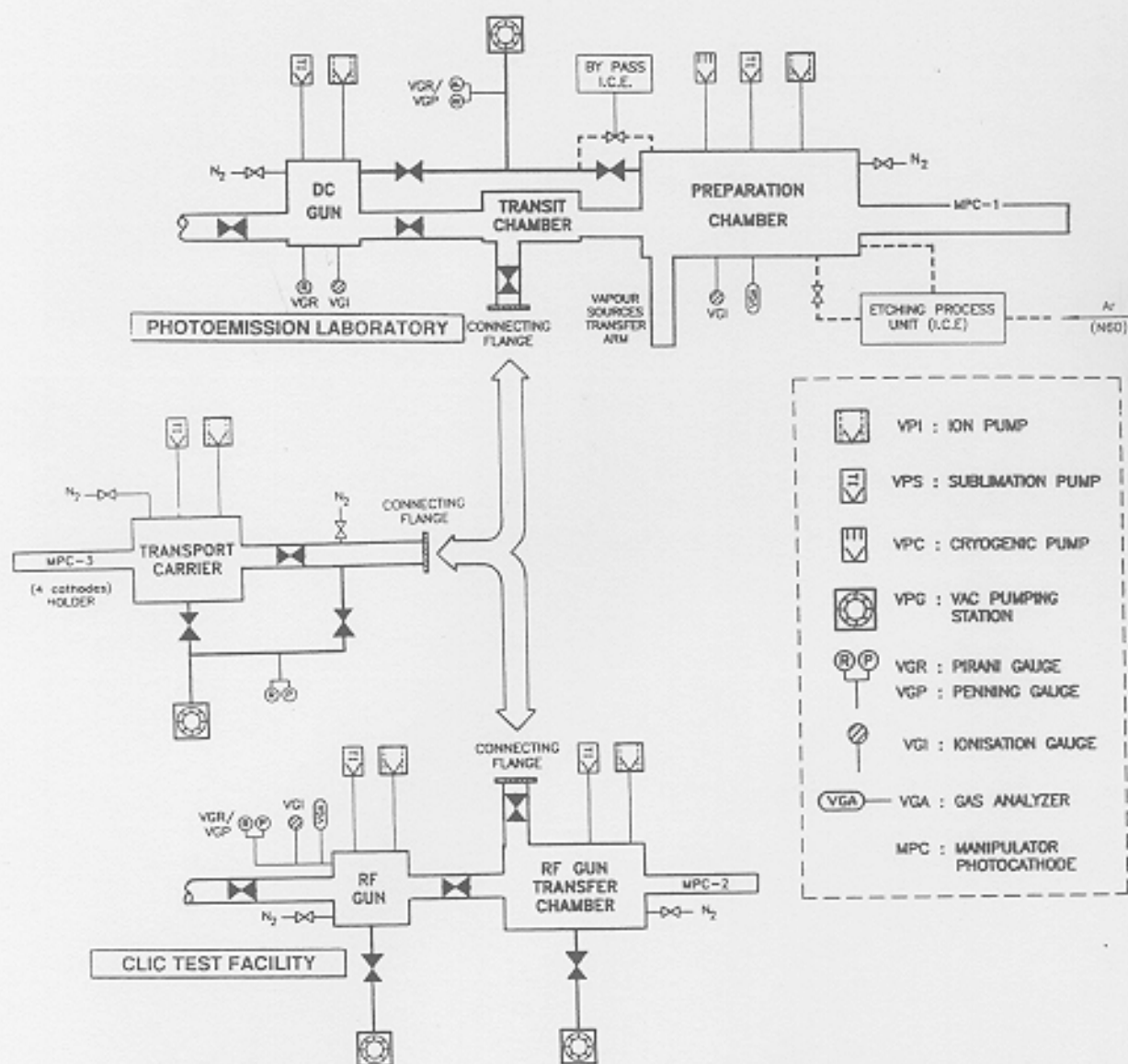

Figure 13:   The photocathode transfer system

produced and tested in the laboratory, and Figure 14 shows for different wavelengths the lifetime of some ones. Cs_2Te cathodes have been optimized at 266 nm, alkali antimonides at 355 nm. During measurements the gun pressure rises from 5×10^{-10} up to 10^{-8} mbar.

specifications. For this reason it was decided to use it in the RF gun. Since the rejuvenation of a Cs_2Te cathode was not conclusive in the CTF, and to avoid the problem of air contamination we need to transport the photocathode under vacuum from the photoemission laboratory to the CTF. The necessary

Table 4: Alkali photocathodes : QE = f(λ)

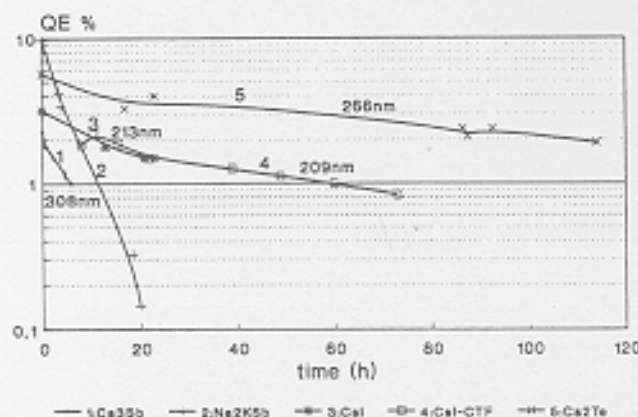| λ (nm)	193	213	266	355	532	Ea + Eg
E (eV)	6.42	5.82	4.66	3.49	2.33	eV
Cs_3Sb		3.5×10^{-2}	2.0×10^{-2}	1.8×10^{-2}	3.8×10^{-3}	2.0
K_3Sb		1.4×10^{-2}	1.6×10^{-2}	7.6×10^{-3}	2.3×10^{-4}	2.3
Na_2KSb		7.7×10^{-2}	6.1×10^{-2}	3.5×10^{-2}	2.0×10^{-4}	2.0
CsI	9.6×10^{-2}	6.8×10^{-2}	7.1×10^{-5}	1.9×10^{-6}		6.4
CsI + Ge		7.3×10^{-3}	1.3×10^{-3}	2.0×10^{-6}		5.0
Cs_2Te		6.0×10^{-2}	5.7×10^{-2}	2.0×10^{-4}		4.5

Figure 14: Alkali photocathode lifetime

equipment is under construction, and we hope to start using this installation before the end of 1993.

7. Acknowledgements

6. Conclusion

In our application, metallic photocathodes have quantum efficiencies which are too low but copper cathodes are useful for debugging the whole CTF installation due to their ease of use. Alkali antimonides have lifetimes which are too short and need very good vacuum. Only alkali halides have demonstrated properties close to CTF specifications. In the CTF, we have used CsI cathodes, with the fifth harmonic of the Nd:YLF laser, because only CsI can withstand exposure to air. As mentioned this wavelength is too impractical, and we have doubts about the relaxation time of this cathode. At present we believe that only Cs_2Te cathodes will meet CTF

Bibliography

1. W. Schnell, *The CLIC Study of an Electron-positron Collider*, CERN SL/92-51 (RFL), CLIC Note 184, paper presented at LC92 ECFA Workshop on e⁺e⁻ Linear Colliders, Garmisch-Partenkirchen, July-August 1992

2. Y. Baconnier, R. Bossart, K.K. Geissler, J.C. Godot, K. Hübner, H. Kugler, J.H.B. Madsen, A.J. Riche, J. Ströde, G. Suberlucq, *The CERN Linear Collider Test Facility (CTF)*, CERN PS 92-49 (LP), Paper presented at the 1992 LINAC Conference, Chalk River, Ontario, Canada, August 23-28, 1992

3. Y. Baconnier, K.K. Geissler, J.H.B. Madsen, A. Pisent, G. Suberlucq, *CLIC STUDIES — The DC test bench for laser driven photo-emissive cathodes*, CLIC Note 116 — CERN/PS 90-24 (LP), Paper presented at the European Particle Accelerator Conference EPAC 90, Nice 12-16 June 1990

4. E. Chevallay, *Contrôle informatisé du processus de fabrication de photocathodes alcalines*, PS/OP Note 93-39, CERN

5. M. Wurgel, *Nettoyage ionique sous vide des Photocathodes*, CERN, PS/LP Note 91-03, CERN January 1991

6. J. Durand, *Utilisation du Wall Current Monitor au Laboratoire de Photoémission PS-LP*, PS/LP Note 91-10, CERN Février 1991

7. Y. Pellégrina, *Coupe de Faraday*, PS/LP Note 89-20, Août 1989

8. E. Chevallay, *Contrôle de mouvement de translation et scrutation automatique de la charge du faisceau emis par une photocathode*, PS/OP Note 93-38, CERN

9. J.H.B. Madsen and L. Rinolfi, *Present status and future of the CERN Linear Collider Test Facility, the CTF*, Paper presented at this conference

10. S.C. Hutchins, *Photocathode lab optical system*, PS/LP Note 93-31, CERN

11. T. Srinivasan-Rao, T. Tsang and J. Fischer, *Photoemission using femtosecond laser pulses*, Brookhaven National Laboratory, Upton, NY 11973, November 1991

12. C. Toth, G. Farkas, D. Charalambidis, E. Hontzopoulos, C. Fotakis, *High brightness electron beam production by laser induced various order multiphoton photoeffect of gold*, Proc. of the Bendor Workshop *Short pulse high current cathodes*, June 18-22, 1990 éditions Frontières France

13. H.B. Michaelson, *The work function of the elements and its periodicity*, Journal of Applied Physics, Vol. 48, No 11, November 1977

14. J.P. Girardeau-Montaut and A. Perez, *Private communications*, Claude Bernard University LYON (France)

15. G. Suberlucq, *Test des photocathodes au laboratoire de photoémission du CERN*, Proceeding of Journées d'Etude sur la Photoémission à Fort Courant, Blaise Pascal University, Clermont-Ferrand (F) April 1992

16. J.H.B. Madsen, *Properties of photocathodes in an RF gun illuminated by ps long laser pulses. Results from experiments in the CERN Linear Collider Test Facility*, Proceeding of "Journées d'Etudes sur la Photoémission à Fort Courant", Observatoire de Paris, April, 1993

17. A.H. Sommer, *Photoemissive materials*, R.E. Krieger Publishing Company Huntington New York, 1980

18. G. Suberlucq, *Photocathodes en iodure de césium utilisées à fort courant*, CLIC Note 162, CERN PS 92-29 (LP), May 1992

19. D. Carminati and A. Braem, *Procédure de fabrication des photocathodes en iodure de césium*, PPE/TA1-TFG Note 91-2, CERN, October 1991

20. T. Tsang, *Private communications*, Brookhaven National Laboratory, Upton N.Y. 11973, July 1991

21. C.I. Coleman, *Imaging detectors for the ultraviolet*, Appl. Optics, vol. 20 No 21, Novembre 1977

22. E. Taft and L. Apker, *Photoemission from Caesium and rubidium tellurides*, J.O.S.A. vol.13 No2, 1953

23. H. Timan, *A survey of recent advances in the theory and practice of vacuum photoemitters*, Advances in Electronics and Electron Physics, Vol. 63, 1985, Academic Press, Inc.

24. C.I. Coleman, *Field enhancement of photoemission from Caesium telluride*, Appl. Optics, vol.17 No11, June 1978